Polymer 50 (2009) 4745–4752

Contents lists available at ScienceDirect

Polymer

journal homepage: www.elsevier.com/locate/polymer

# Composition effect on dewetting of ultrathin films of miscible polymer blend

Jichun You [a], Shanshan Hu [a], Yonggui Liao [b], Kaixu Song [a], Yongfeng Men [a], Tongfei Shi [a,*], Lijia An [a,*]

[a] State Key Laboratory of Polymer Physics and Chemistry, Changchun Institute of Applied Chemistry, Chinese Academy of Sciences, Changchun 130022, China
[b] School of Chemistry and Chemical Engineering, Huazhong University of Science and Technology, Wuhan 430074, China

ARTICLE INFO

*Article history:*
Received 19 May 2009
Received in revised form
3 July 2009
Accepted 1 August 2009
Available online 5 August 2009

*Keywords:*
Composition fluctuation
Dewetting
Polymer blend

ABSTRACT

Two kinds of dewetting and their transition induced by composition fluctuation due to different composition in blend [poly(methyl methacrylate) (PMMA) and poly(styrene-ran-acrylonitrile) (SAN)] films on $SiO_x$ substrate at 145 °C have been studied by in-situ atomic force microscopy (AFM). The results showed that morphology and pathway of dewetting depended crucially on the composition. Possible reason is the variation in intensity of composition fluctuation resulted from the change of components in polymer blend. Based on the discussion of this fluctuation due to the composition gradient, parameter of $U_{q0}/E$, which describes the initial amplitude of the surface undulation and original thickness of film respectively, has been employed to distinguish the morphologies of spontaneous dewetting including bicontinuous structures and holes. Prior to the investigation of dewetting, it is confirmed that this blend is miscible at 145 °C using grazing incidence ultra small-angle X-ray scattering (GIUSAX).

© 2009 Elsevier Ltd. All rights reserved.

## 1. Introduction

Dewetting of polymer ultrathin films is an important topic because understanding of its physical nature is the key to many applications, such as coating techniques, adhesives, lubrication, microelectronics and biophysics [1–6]. Polymer has been used widely as models to study dewetting due to two advantages. One is that the vapor pressure of polymer is negligible and thus the mass of the film is conserved; the other is the time resolution for the low mobility of polymer chains [7,8]. Therefore, there are many reports on dewetting of polymer ultrathin films and exist several dewetting mechanisms including spinodal dewetting, nucleation and growth, autophobicity and density fluctuation [6]. However, most of these reports focused on single-component polymer films on different substrates [8–14], such as silicon wafer, glass, mica, self-assembled monolayer or grafted substrate, patterned substrate, or one component on top of another.

Recently, dewetting in polymer blend films has attracted many interests for popular applications as well as fundamental investigations [15–18]. However, much attention has been paid to phase-separated systems (two-phase region). These systems may involve the competition between phase separation and dewetting [19], which arouses complicated phase behavior in polymer blend film. For instance, Tanaka et al. [20] and Oron et al. [21] found that a bilayer film formed and then the upper layer dewetted on the lower layer because phase separation occurred much earlier than dewetting. Our previous work [7] showed that dewetting of the whole film occurred firstly and then phase-separation appeared in the dewetted droplets accompanied by wetting of PMMA on the substrate when dewetting took place earlier than phase separation. Unfortunately, dewetting of miscible polymer blend film is far away from understanding, which is the base of investigations of complicated phase behavior between phase separation and dewetting. Therefore, it is necessary to explore dewetting of polymer blend films in one-phase region.

In 2002, Wensink and Jérôme [22] indicated that composition fluctuation can induce dewetting of miscible polymer blend films. They theoretically investigated dewetting of single-component films due to density fluctuation, which was further studied by Sharma et al. [23], and predicted that the composition fluctuation in blend films, similar to density fluctuation in single-component films, would induce dewetting of miscible polymer blend films. In addition, it is obvious that amplitude of composition fluctuation, which relies on composition of polymer blend, has much effect on dewetting process. However, it is obscure how compositions of polymer blend affect dewetting. Therefore, it is significant to investigate the process of dewetting with various compositions in one-phase region. To our knowledge, however, there is no report on this.

In our present work, we investigated dewetting of ultrathin film of miscible PMMA/SAN blend with different composition by AFM and GIUSAX. It was found that dewetting process strongly depended on the composition of polymer blend. Growth of dewetted structures in this mechanism has been investigated in detail. Based on the discussion of intensity of composition fluctuation, parameter of $U_{q0}/E$

* Corresponding authors. Tel.: +86 431 85262137/+86 431 85262206; fax: +86 431 85262969/+86 431 85685653.
*E-mail addresses:* tfshi@ciac.jl.cn (T. Shi), ljan@ciac.jl.cn (L. An).

0032-3861/$ – see front matter © 2009 Elsevier Ltd. All rights reserved.
doi:10.1016/j.polymer.2009.08.002

in reference [22] was employed to distinguish morphologies of dewetting including bicontinuous structure and holes.

## 2. Experiment

The polymer system is a blend of poly(methyl methacrylate) (PMMA) (Mw = 387 kg/mol, PD = 3.72) and poly(styrene-ran-acrylonitrile) (SAN) (Mw = 149 kg/mol, PD = 2.66, 30 wt% of AN) purchased from Across and Aldrich respectively. SAN was purified by method discussed elsewhere [24]. The glass transition temperatures of PMMA and SAN are 119.5 °C and 112.0 °C, respectively (from DSC, data not shown). Thin blend films were prepared by spin-coating 1,2-dichloroethane solution (0.1 g/ml) of PMMA/SAN (50:50, 30:70 and 10:90 wt%) onto the silicon wafer. Three samples labeled as SAN50, SAN70, and SAN90 were obtained respectively. Prior to spin-coating, the silicon wafers were cleaned in a bath of 100 ml of 80% $H_2SO_4$, 35 ml of 30% $H_2O_2$, and 15 ml of deionized water at 80 °C for 60 min and rinsed in deionized water, then blown-dried with compressed nitrogen. Thickness of all our films measured by a D8 Discover X-ray reflectometer (Bruker, Germany) was 9.7 ± 0.2 nm.

The in-situ topography images were obtained using an SPA-300 HVA (Seiko Instruments Inc., Japan) at 145 °C with a temperature-control stage driven in tapping mode [7]. A silicon tip (Olympus, Japan) with a spring constant of 42 N/m was used. Synchrotron GIUSAX measurements were performed at the BW4 beamline at HASYLAB (Hamburg, Germany), using a monochromatic X-ray beam with energy of 8.979 keV. The sample to detector distance was $L = 13\,037$ mm. The incident angle is 0.3°. X-ray scattering intensity patterns were acquired by a two-dimensional detector array (2048 × 2048 pixels). Prior to measurement of GIUSAX, two samples of SAN50 were annealed at 145 °C and 155 °C for 60 h in oven respectively.

## 3. Results and discussion

Firstly, it is necessary to assess the miscibility of PMMA/SAN in the blend film. GIUSAX, a powerful scattering technique, by which we can detect the large-size dewetted droplets and small size phase-separated structures in this kind of droplets, was employed to measure structures in our films. Measurements of (micro-)phase-separated structures in co-polymer and polymer blend by means of GIUSAX (or GISAXS, GISANS) have been validated by many systems such as PS/PpMS [15], PS-b-PI [25], PS-b-PEO [26], etc. [27–32]. In literature [15], Müller-Buschbaum got the phase-separated structures in dewetted droplets (similar with our imagination to the structures), suggesting that it is possible to confirm this kind of structures by means of GIUSAX in our experiment. Furthermore, there is enough contrast of electronic density in our system since densities of PMMA and SAN are 1.17 g/cm$^3$ and 1.08 g/cm$^3$, respectively. Therefore, GIUSAX of two samples (annealed at 145 °C and 155 °C for 60 h respectively) was carried out. Fig. 1A and B show the two-dimensional intensity distribution of SAN50 annealed at 155 °C and 145 °C, respectively. Fig. 1C gives the common double logarithmic presentation in reciprocal space. There are two peaks at $q_y = 0.015$ nm$^{-1}$ and $q_y = 0.073$ nm$^{-1}$ respectively (corresponding to two kinds of ordered structure in the polymer blend film) for the sample annealed at 155 °C for 60 h (solid line in Fig. 1C). On the other hand, characteristic wave vector of Fig. 1D in reference [7] (the same annealing temperature and approximative time with the specimen in GIUSAX) is $q = 0.018$ nm$^{-1}$ by 2D fast Fourier transform (FFT), which is in good agreement with that in GIUSAX, suggesting that $q_y = 0.015$ nm$^{-1}$ is a representation of the correlation length (about 418 nm) of droplets on the substrate. There are two possible reasons for the other peak at $q_y = 0.073$ nm$^{-1}$. One is that this peak is the representation of the correlation among the smaller droplets in AFM topography images and the other is that there is phase-separated

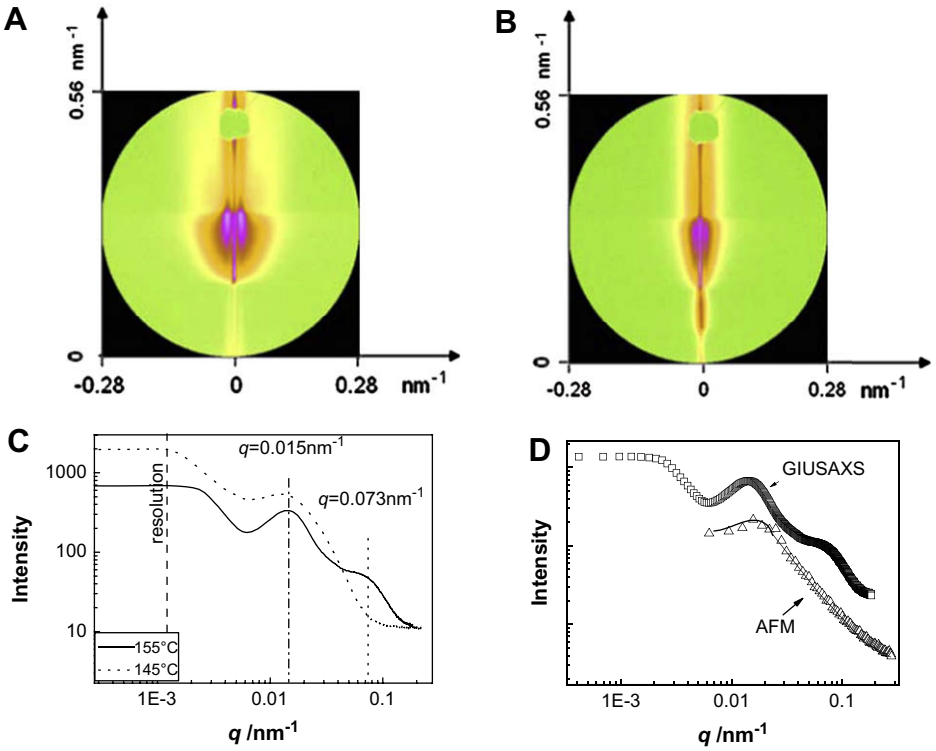


**Fig. 1.** Two-dimensional intensity distribution of the sample SAN50 annealed at (A) 155 °C and (B) 145 °C respectively. (C) The common double logarithmic presentation in reciprocal space. The solid and dotted lines are the results of SAN50 annealed at 155 °C and 145 °C respectively. (D) Comparison between the master curves calculated from the AFM data (triangle) and the GIUSAX data (square) at 155 °C.

structure of PMMA- and SAN-rich phases in droplets. In Fig. 1D, the mean distance between the droplets gives rise to the only structure (triangle in Fig. 1D) factor peak at $q = 0.016\ \mathrm{nm}^{-1}$, implying an illegitimate explanation as smaller droplets for peak at $q_y = 0.073\ \mathrm{nm}^{-1}$ in GIUSAX. Therefore, this structure must be composed of the two components of PMMA and SAN. In other word, phase separation takes place in the film and ordered structures of PMMA- and SAN-rich phases form [33], which is similar to the method (Fig. 3D in reference [15]) introduced by Müller-Buschbaum to detect phase and microphase-separated structure in dewetted droplets [15]. For the sample annealed at 145 °C (dotted line in Fig. 1C), there is only one peak at $q_y = 0.015\ \mathrm{nm}^{-1}$ which denotes the same meaning as that of sample at 155 °C. According to above discussion, it is confirmed that phase separation takes place at 155 °C and does not take place at 145 °C for SAN50 films with a thickness of 9.7 nm. This critical point temperature is much lower than that in the bulk (165 °C) [34]. This decrease of temperature comes from the confinement resulted from the decrease of film thickness [20]. In our previous work [7], the film of PMMA/SAN blend was treated as a miscible system at 155 °C due to the limitation of AFM on internal structures. Similarly, GIUSAX data indicates that there is no phase-separated structure at 145 °C for the sample of SAN70 and SAN90 (data not shown here).

On the basis of confirmation of miscibility, we can investigate dewetting process of SAN50, SAN70 and SAN90. Fig. 2 shows topography images and line cut of SAN50 film annealed at 145 °C for different time. The bicontinuous surface patterns (Fig. 2A–C) appear seemingly similar to the spinodal decomposition patterns found in phase separation. Initially, some slight amplitude bicontinuous structures including long hills and gullies appear. For the sake of coalescence, the hills and gullies grow in width and height with time (Fig. 2A–C) [12,14]. After continuous long hills decay into droplets (highlighted with ellipse in Fig. 2D–F), these droplets become rounder and rounder due to the surface tension and develop in height noteworthily (Fig. 2F). Finally, droplets with larger diameters form after growth and merger of them. This scenario is in good agreement with the result of phase-separated specimen at 175 °C and 185 °C [24,33,34].

In order to obtain the amplitude of surface undulation, our attention is paid to the root-mean-square surface smoothness (RMS) of topography images in AFM, which is the reflection of amplitude in these images. If the surface undulation is treated as the simplest sine or cosine equation, we can get the linear relationship between the amplitude ($U_q$) and RMS as $U_q = (\pi/2)\mathrm{RMS}$. According to the discussion above, the annealing time dependences of the amplitude and the character wave number of composition fluctuation on a log–log scale are shown in Fig. 3. RMS of as-prepared film before a temperature jump is not shown here due to little difference between them. In Fig. 3A, $U_q$, as a function of annealing time, exhibits three distinct regimes. Namely, $U_q$ follows a power law of $t^{0.17}$ in the early stage and $t^{0.35}$ in the later stage, then a slowing down from fast growth occurs [34]. Three regimes cross

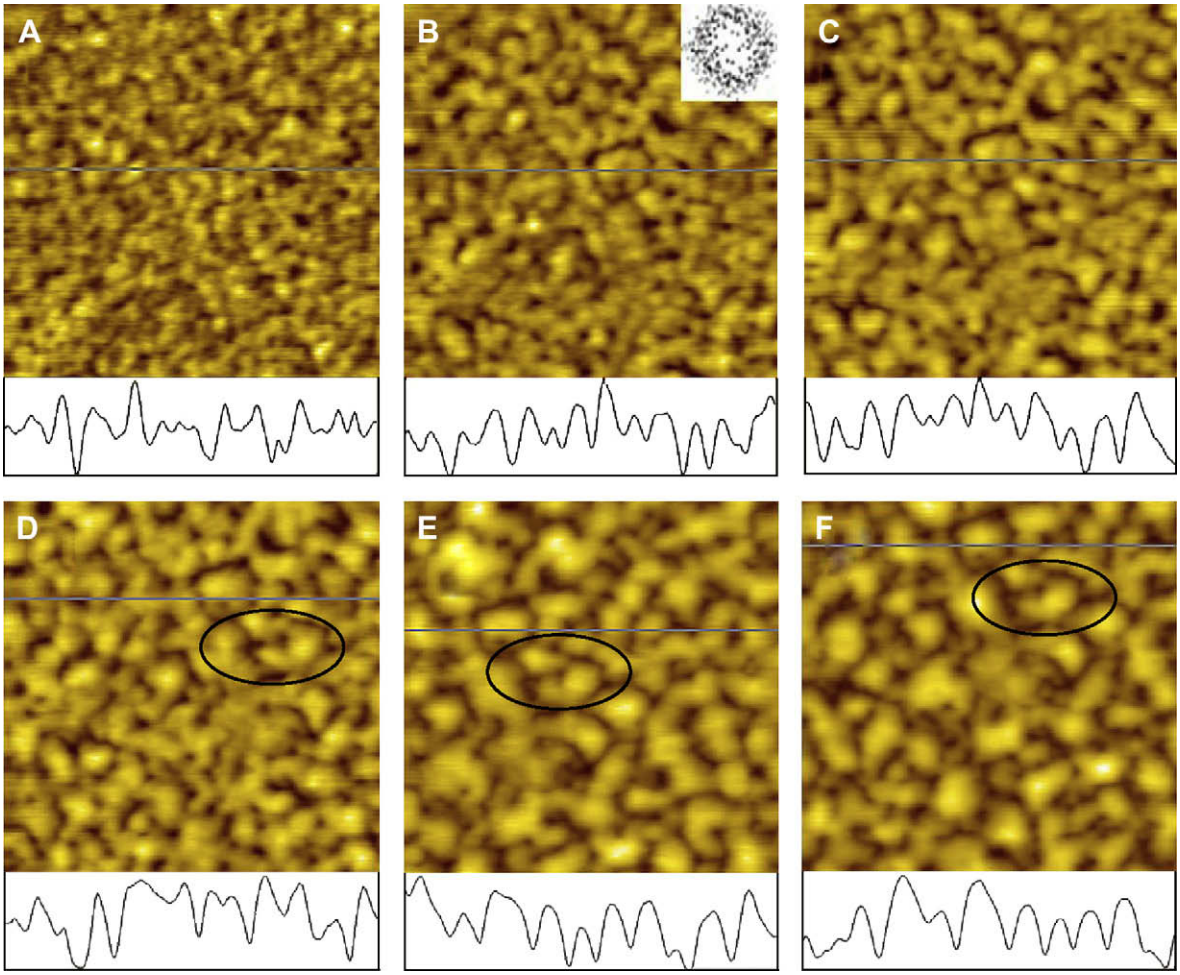


**Fig. 2.** Snapshots of topography images and line cut for sample of SAN50 at 145 °C for (A) 9 min, (B) 52 min, (C) 124 min, (D) 202 min, (E) 1280 min, and (F) 2806 min. The dimensions and the *Z*-axes values for topography images are $2 \times 2\ \mu\mathrm{m}^2$ and 10.8 nm respectively. Inset in image B is the fast Fourier transition (FFT) of corresponding image.

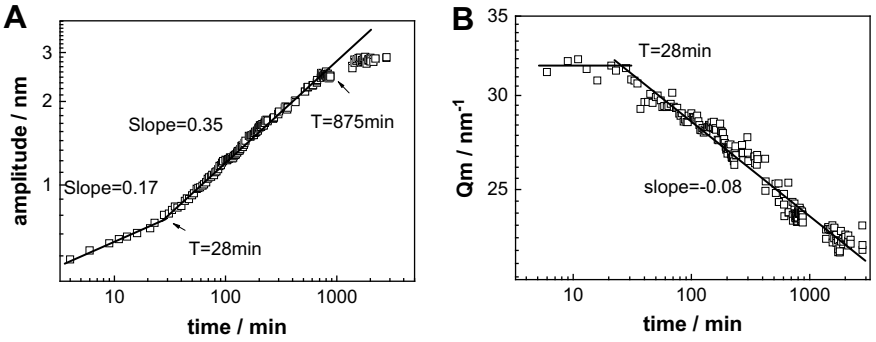


**Fig. 3.** Annealing time dependence of (A) amplitude and (B) character wave number of surface undulation for SAN50 at 145 °C.

at ~28 min and at ~875 min respectively. This is different from dewetting of polystyrene (PS) on the substrate of $SiO_x$ [9,12], in which the amplitude grows exponentially in the initial stage in accord with the prediction of the spinodal dewetting model [35,36]. This difference may come from the influence of the composition gradient due to diffusion of PMMA to the substrate. The plot of log $Q_m$ versus log $t$ (Fig. 3B) suggests two distinct stages of dewetting process. In the early stage, character wave numbers is independent with annealing time, which implies that the period of the surface undulation remains constant. In the second stage, the exponent of power law is near −0.08. Two regimes cross at ~28 min, the same time as the evolution of amplitude. This exponential estimate is different from −1/3 controlled by diffusion and −0.43 for polystyrene on $SiO_x$ substrate [7,12]. With the help of combination of amplitude and character wave numbers, it is easy for us to describe the surface undulation in detail. At the beginning, along with the form of undulation, amplitude grows slowly while period remains constant. After 28 min, both of them increase rapidly. Finally, growth of amplitude slows down and deviates from the power law at ~875 min and then tends to a certain value [34], while period grows still since decrease of character wave numbers continues. Three stages discussed above are seemingly similar to

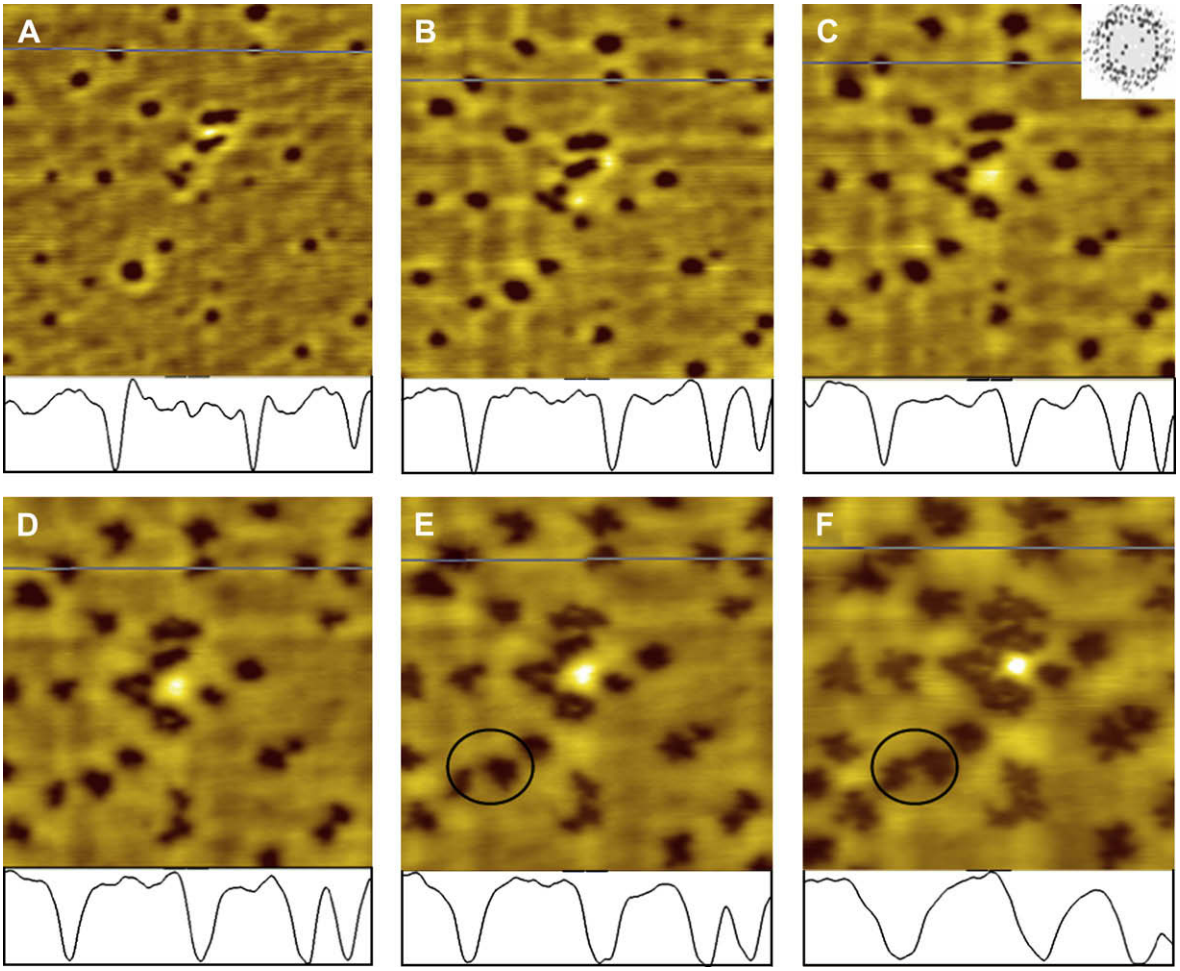


**Fig. 4.** Snapshots of topography images and line cut for sample of SAN90 at 145 °C. Sample is annealed for 22 min (A), 98 min (B), 222 min (C), 537 min (D), 1209 min (E) and 4740 min (F). The dimensions and the $Z$-axes values for topography images are $2 \times 2\ \mu m^2$ and 18.2 nm respectively. Inset in image C is the fast Fourier transition (FFT) of that image.

early, inter and late stage in the spinodal decomposition of polymer blend [37].

Fig. 4 shows the pattern evolution of SAN90 at 145 °C. Occurrence and development of holes are completely different (both in AFM images and line cut) from the growth of bicontinuous structures of SAN50 in Fig. 2. So above process is considered as a new mechanism of "expansion of holes". Shown in Fig. 4A, some holes with diameters close to 100 nm, which are surrounded by an increasing thick uneven circular rim, distribute over the surface. During the holes growth, the number does not increase remarkably (Fig. 4B and C). After the sample annealed at 145 °C for ~537 min (Fig. 4D), shape of some holes changes from circular to polygonal due to different growth velocities in different directions, which is in accord with the reported result of theory [35] and experiment [38,39]. This evolution is repeated by more and more holes during their development. Growing further, these holes have no choice but to merge with each other for increasing area (highlighted by ellipse in Fig. 4E and F), which is followed by the formation of droplets as expected.

Is there any law during the growth of hole diameters? In Fig. 5A, diameters in certain direction of three holes (e.g. hole 1, 2 and 3) are investigated and the developments of them are exhibited in Fig. 5B. For diameter of hole 1 (D1 in Fig. 5B), following rapid increase initially, a slowing down occurs. However in hole 2 and 3 (D2 and D3), they increase with annealing time linearly and velocities of this growth are different. In addition, diameters of the same hole in the direction of X (solid line in Fig. 5A) and Y (dash line in Fig. 5A) increase in two distinct ways too. In one word, there is so great difference in growth of diameters in different holes (data of other holes not shown here) or even in different directions of the same hole that evolution of diameters is unsuitable to describe the hole growth, which is not in accord with the development of hole diameters in Nucleation and Growth (NG) [40,41]. Then ratio of $S_{hole}/S_{all}$ (area of holes and the whole scan area, respectively) is introduced to describe the evolution of these holes since number of holes does not increase remarkably. In Fig. 5D, there are two stages of this ratio growth during dewetting of SAN90. It is obvious that the average exponent of diameter growth is 0.075 in the early stage and 0.23 in the later stage due to the quadratic relationship between the diameter and area. Both of them are smaller than the predicted values, which are 1 and 2/3 for films with different thickness [42]. It is noted that interaction between polymer and substrate plays an important role in diffusion of rims [35]. Slow diffusion results from the strong interaction. For PMMA/SAN films in this case, the reason for lower exponent is that the attractive interaction between PMMA wetting layer close to substrate and the upper blend layer is so strong [6].

Fig. 6 shows a mixed process of "expansion of holes" and "fragmentation of bicontinuous structures" in the specimen of SAN70. In Fig. 6A, both holes and surface undulations are clear enough [12]. The expansion of holes and the coalescence of bicontinuous structure are performed simultaneously during anneal. However, these holes grow in height so much that bicontinuous structure is invisible (Fig. 6B). Along with the growth of these holes in height and diameter, some "new" holes with smaller diameters appear (Fig. 6B and C). As a result, the number of holes per unit area increases and merger of these holes is unavoidable. This kind of merger of several neighboring holes in certain direction isolates the film surrounded by them and produces some islands (highlighted by ellipse in Fig. 6A–D). Then these islands become increasingly circular (Fig. 6E and F) and merge with each other due to the Laplace pressure [43].

Fig. 7A shows the annealing time dependence of $S_{hole}/S_{all}$ ratio. The early exponent of power law becomes 1.65, much larger than that in SAN90 due to the notable increase of hole number. Then this ratio is the representation of not diameter growth but the coupling of the increase of the area of each hole and the number of holes. Evolution of hole number is shown in Fig. 7B. It increases from 29 to 113 and 23 to 31 for specimen of SAN70 and SAN90 respectively and then remains constant. It is evident that change of hole number is more remarkable in SAN70, suggesting that the contribution of increase of hole number per unit area to the appearance of dewetting cannot be negligible.

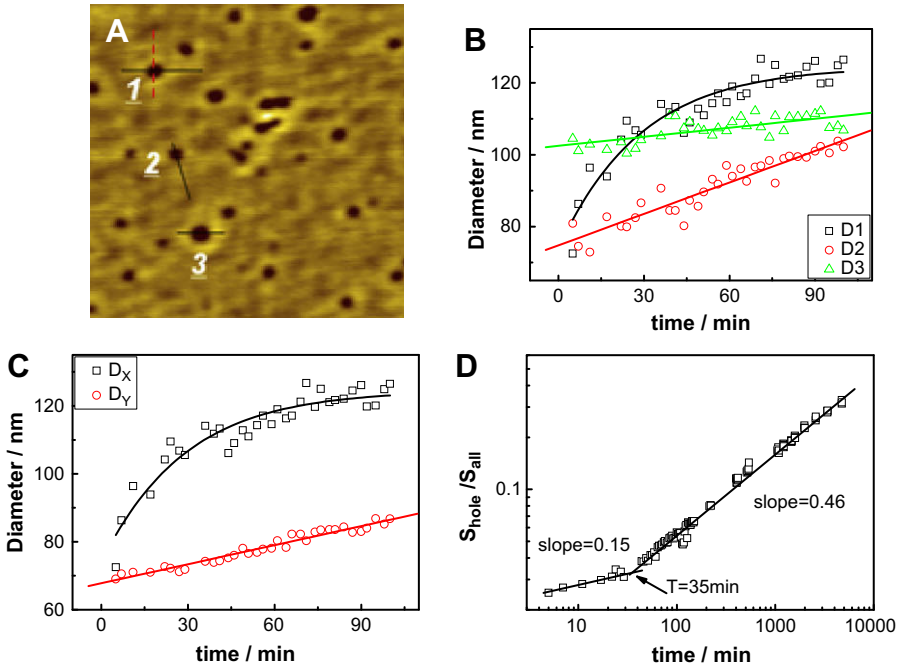


**Fig. 5.** (A) AFM topography image of SAN90 annealed at 145 °C for 22 min. (B) Annealing time dependence of diameter, hole 1, 2 and 3 corresponding to the hole shown in (A). (C) Annealing time dependence of diameter of hole 1 in the two directions, *X* and *Y*. (D) Annealing time dependence of the ratio of hole areas to the whole scan area (For interpretation of the references to color in this figure legend, the reader is referred to the web version of this article.).

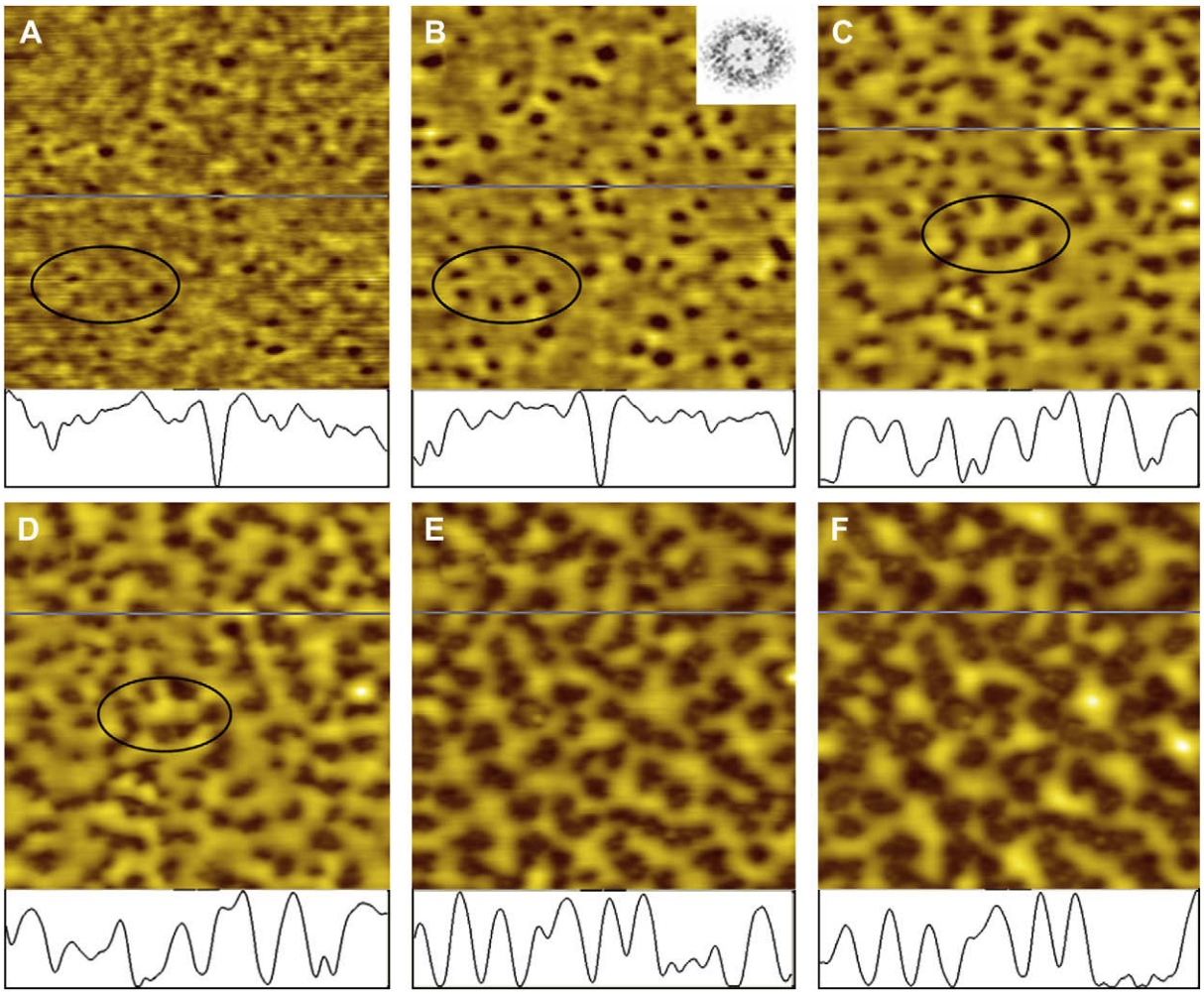


**Fig. 6.** Snapshots of topography images and line cut for sample of SAN70 at 145 °C for 33 min (A), 91 min (B), 287 min (C), 460 min (D), 1121 min (E) and 3144 min (F). The dimensions and the *Z*-axes values for topography images are $2 \times 2\ \mu m^2$ and 22.4 nm respectively. Inset in image B is the fast Fourier transition (FFT) of corresponding image.

PMMA/SAN is a typical lower critical solution temperature (LCST) system. It has been proved by many reports that attractive interaction between PMMA and $SiO_x$ is stronger than that of SAN [7,34]. Furthermore, both PMMA and SAN films wet the substrate of $SiO_x$ well [7]. In light of above discussion, we can apply the idea of composition fluctuation to our system since it matches the conditions of this theory completely [22]. Moreover, our previous work [7] has proved that composition fluctuation appeared in PMMA/SAN blend film at 155 °C and 175 °C. Due to the miscibility of PMMA/SAN at room temperature, the spin-coated film is homogeneous. When the sample is heated to 145 °C (above $T_g$), PMMA diffuses to the substrate because of the more favorable interaction with $SiO_x$, leading to a gradient of PMMA composition across the film (in the direction of film thickness). Composition fluctuation will appear due to the non-uniformity of this gradient, which is the right reason for dewetting by the mechanism of composition fluctuation. It must be noticed that component (PMMA or SAN) diffusing to surface will affect this fluctuation. In our system, however, PMMA and SAN have nearly equal surface tension at this temperature [44]. Therefore, it is reasonable to ignore this effect. In addition, it is clear that there are some difference from and also some similarities to the results of spinodal dewetting in one component polymer thin films in above

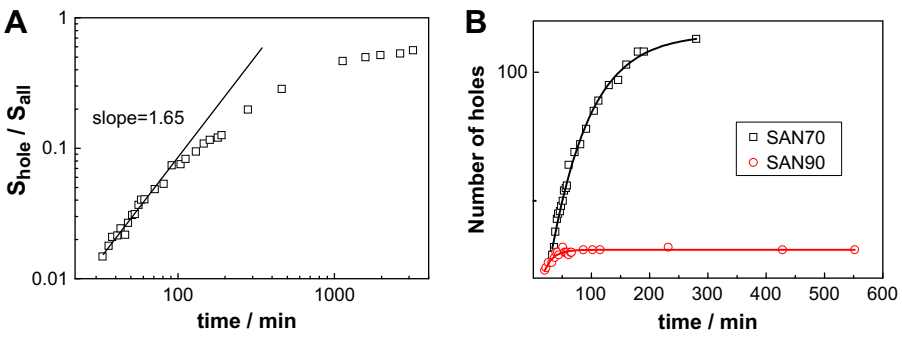


**Fig. 7.** Annealing time dependence of the ratio of hole areas to the whole scan area (A) and number of hole (B).

process [12,45]. Qualitatively, development of period and amplitude of surface undulation seems similar to three stages of spinodal dewetting and spinodal decomposition in phase separation. However, velocities of growth of holes in SAN90 and variation of character wave numbers in SAN50 have lower magnitude due to the strong interaction between the PMMA wetting layer and upper blend layer.

It is very interesting that dewetting pathway of polymer blend ultrathin films induced by composition fluctuation is similar to that of spinodal dewetting of single-component investigated by simulation [13,14]. In those reports, simulations were carried out on PS films with different thickness. Two kinds of completely different pathway and a transition between them were found. In the first pathway, the occurrence of dewetting resulted from the fragmentations of bicontinuous structures and retractions of droplets. In the second one, however, pattern evolution was achieved by significant expansion of holes and polygonal structures. In the transitional sample with intermedial thickness, this bicontinuous patterns resolved into a mixture of both holes and drops in varying proportions depending on the initial thickness of the film. These three pathways in the results of simulation [13,14] are in good agreement with our results of SAN50, SAN90 and SAN70, respectively. In addition, occurrence of droplets in the pathway of "fragmentation of bicontinuous structures" is earlier than that of "expansion of holes" in simulation [13,14] and experiment [12]. This law works well still in PMMA/SAN blend films in both our previous [46] and this work (Figs. 2D, 4C and 6C). These similarities on morphology and velocity of dewetting between composition fluctuation (our experiment) and spinodal dewetting (simulation and experiment on PS films) come from the relativity of them [23,47–49].

From above discussion, it can be seen that two kinds of pattern evolution in PS films reoccur in our AFM images of polymer blend ultrathin films. In simulation based on 3D nonlinear equation, Sharma and Khanna [13,14] ascribed different pathways to the form of the intermolecular potential in an extended neighborhood of the initial thickness. However, what is the reason for the plenty of morphologies of dewetting induced by composition fluctuation in our system since thickness of these films is nearly equal? To distinguish the pathway in spontaneous dewetting, parameter of $U_{q0}/E$, where $U_{q0}$ and $E$ describe the initial amplitude of the surface undulation and the original film thickness [12,22] respectively, is introduced in light of the existence of composition gradient and intensity of fluctuation [22]. In our blend system, composition fluctuation appears because of the non-uniformity of composition gradient. Intensity of this kind of fluctuation depended crucially on the composition as shown in Fig. 8. A fit and extrapolation of the data in Fig. 8 indicate that the initial amplitude of the surface undulation of SAN50 is higher than that of SAN90 at the same temperature of 145 °C, namely, $(U_{q0})_{SAN50} > (U_{q0})_{SAN70} > (U_{q0})_{SAN90}$, i.e., $(U_{q0}/E)_{SAN50} > (U_{q0}/E)_{SAN70} > (U_{q0}/E)_{SAN90}$ (all the samples have nearly equal thickness in this work). Thus a rule can be found that for film with higher magnitude of $U_{q0}/E$, it dewets by means of "fragment of bicontinuous structure" (pathway of SAN50 shown in Fig. 2), while for film with lower magnitude of $U_{q0}/E$, it undergoes the way of "expansion of holes" (pathway of SAN90 shown in Fig. 4). Since change of either $U_{q0}$ or $E$ can result in the variation of this ratio and the rule works well in the case of samples having the same $E$ but different $U_{q0}$, it should also be valid in the case of samples with the different $E$ but the same $U_{q0}$. Is that true? This can be validated in the system with approximative $U_{q0}$ [50] and different $E$ in films composed of one component (PS) [14] and blend (PMMA/SAN) [46]. Indeed, pathways of dewetting in PS films (with thickness of 7 nm – fragment of bicontinuous structure, 8.5 nm – transitional pathway and 13 nm – expansion of holes) [14] and PMMA/SAN films (with thickness of 8.7 nm – fragment of bicontinuous structure, 39.8 nm – transitional pathway and 50.4 nm – expansion of holes) [46] indicate that the new parameter works well. Thus the conclusion can be drawn that variation in thickness and composition in polymer blend films have equivalent effect on pathway of spontaneous dewetting and $U_{q0}/E$ is an effective parameter to distinguish the morphologies and pathway of dewetting in films with different original thickness or different component. Qualitatively, intensity of composition fluctuation of SAN50 is strong since it is near critical composition. That is, fraction of PMMA is sensitive to the diffusion of itself, resulting in higher $RMS_0$, $U_{q0}$ and $U_{q0}/E$. Therefore the amplitude is comparable with film thickness in SAN50. It is easier to dewet by its original way of bicontinuous structures. In SAN90, however, it is difficult to diffuse to the substrate for PMMA due to the low amount of it. Holes, resulted from many puny bicontinuous structures, come into being and develop. In one word, different composition in blend leads to different intensity of composition fluctuation, which is the reason for different dewetting pathway.

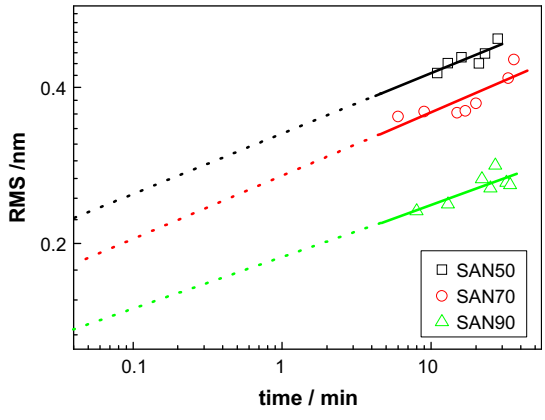


**Fig. 8.** Annealing time dependence of RMS and its extrapolation for SAN50, SAN70 and SAN90 at 145 °C.

## 4. Conclusion

Using grazing incidence ultra small-angle X-ray scattering (GIUSAX), phase-separated structures in dewetted droplets are detected at 155 °C while PMMA/SAN is miscible at 145 °C in films with original thickness of about 9.7 nm. Based on this, two kinds of pathway and their transition of dewetting induced by composition fluctuation were studied. The results show that morphologies and pathway of dewetting depend crucially on the composition. Furthermore, growth of dewetted structures in our results follows different law relative to that in single-component films. The parameter of $U_{q0}/E$ is introduced to distinguish morphologies and pathways of dewetting. It works well for polymer blend films and polystyrene films on $SiO_x$ both in simulation and experiment. Our results are significant for controlling the evolution of dewetting patterns and further understanding of complicated phase behavior including phase separation and dewetting.

## Acknowledgement

This work is supported by the National Natural Science Foundation of China (50503022) Programs and the Fund for Creative Research Groups (50621302), and subsidized by the Special Funds for National Basic Research Program of China (2003CB615600). L.J. An also thanks the supports from the NSFC (20674086, 50390090) and HASYLAB project II-20052011. We thank Dr. A. Timmann and Dr. S.V. Roth assistance in GIUSAX at HASYLAB.

## Reference


[1] Glasner KB, Witelski TP. Phys Rev E 2003;67:016302.
[2] Wang L, Hong S, Hu HQ, Zhao J, Han CC. Langmuir 2007;23:2304.
[3] Vix ABE, Müller-Buschbaum P, Stocker W, Stamm M, Rabe JP. Langmuir 2000; 6:0456.
[4] Bauer E, Maurer E, Mehaddene T, Roth SV, Müller-Buschbaum P. Macromolecules 2006;39:5087.
[5] Reiter G. Phys Rev Lett 2001;87:186101.
[6] Geoghegan M, Krausch G. Prog Polym Sci 2003;28:261.
[7] Liao YG, Su ZH, Sun ZY, Shi TF, An LJ. Macromol Rapid Commun 2006;27:351.
[8] Reiter G. Phys Rev Lett 1992;68:75.
[9] Müller-Buschbaum P. J Phys Condens Matter 2003;15:R1549.
[10] Seemann R, Herminghaus S, Jacobs K. Phys Rev Lett 2001;86:5534.
[11] Reiter G. Langmuir 1993;9:1344.
[12] Xie R, Karim A, Douglas JF, Han CC, Weiss RA. Phys Rev Lett 1998;81:1251.
[13] Sharma A, Khanna R. Phys Rev Lett 1998;81:3463.
[14] Sharma A, Khanna R. J Chem Phys 1999;110:4929.
[15] Müller-Buschbaum P, Gutmann JS, Stamm M, Cubitt R, Cunis S, von Krosigk G, et al. Physica B 2000;283:53.
[16] Müller-Buschbaum P, Gutmann JS, Stamm M. Macromolecules 2000;33:4886.
[17] Müller-Buschbaum P, O'Neill SA, Affrossman S, Stamm M. Macromolecules 1998;31:5003.
[18] (a) Ogawa H, Kanaya T, Nishida K, Matsuba G. Polymer 2008;49:254;
(b) Ogawa H, Kanaya T, Nishida K, Matsuba G. Polymer 2008;49:2553.
[19] Clarke N. Macromolecules 2005;38:6775.
[20] Tanaka K, Yoon JK, Takahara A, Kajiyama T. Macromolecules 1995;28:934.
[21] Oron M, Kerle T, Yerushalmi-Rozen R, Klein J. Phys Rev Lett 2004;92:236104.
[22] Wensink KDF, Jérôme B. Langmuir 2002;18:413.
[23] Sharma A, Mittal J, Verma R. Langmuir 2002;18:10213.
[24] Newby BZ, Composto RJ. Macromolecules 2000;33:3274.
[25] Müller-Buschbaum P. Anal Bioanal Chem 2003;376:3.
[26] Sun Z, Wolkenhauer M, Bumbu GG, Kim DH, Gutmann JS. Physica B 2005; 357:141.
[27] Müller-Buschbaum P, Cubitt R, Petry W. Appl Phys A 2002;74:s342.
[28] Müller-Buschbaum P, Gutmann JS, Cubitt R, Stamm M. Colloid Polym Sci 1999;277:1193.
[29] Zeng YW, Tian CG, Liu JL. Mat Sci Eng B 2006;128:63.
[30] Lee B, Yoon J, Oh W, Hwang Y, Heo K, Jin KS, et al. Macromolecules 2005; 38:3395.
[31] Müller-Buschbaum P, Cubitt R, Petry W. Langmuir 2003;19:7778.
[32] Müller-Buschbaum P, Gutmann JS, Cubitt R, Petry W. Physica B 2004; 350:207.
[33] Liao YG, Su ZH, Ye XG, Li YQ, You JC, Shi TF, et al. Macromolecules 2005;38:211.
[34] (a) Wang H, Composto RJ. Interface Sci 2003;11:237;
(b) Wang H, Composto RJ. Macromolecules 2002;35:2799.
[35] Wyart FB, Daillant J. Can J Phys 1990;68:1084.
[36] Milchev A, Binder K. J Chem Phys 1978;1997:106.
[37] Paul DR, Newman S, editors. Polymer blend. New York: Academic Press; 1978.
[38] Peng J, Xuan Y, Wang HF, Li BY, Han YC. Polymer 2005;46:5767.
[39] Masson JL, Olufokunbi O, Green PF. Macromolecules 2002;35:6992.
[40] Segalman RA, Green PF. Macromolecules 1999;32:801.
[41] Qu S, Clarke CJ, Liu Y, Rafailovich MH, Sokolov J, Phelan KC, et al. Macromolecules 1997;30:3640.
[42] Redon C, Brzoska JB, Brochard-Wyart F. Macromolecules 1994;27:468.
[43] Neto C, Jacobs K, Seemann R, Blossey R, Becker J, Grün G. J Phys Condens Matter 2003;15:3355.
[44] You JC, Shi TF, Liao YG, Li XL, Su ZH, An LJ. Polymer 2008;49:4456.
[45] Seemann R, Herminghaus S, Jacobs K. J Phys Condens Matter 2001;13:4925.
[46] Liao YG, You JC, Shi TF, An Lj, Dutta PK. Langmuir 2007;23:11107.
[47] Sharma A, Mittal J. Phys Rev Lett 2002;89:186101.
[48] Kaya H, Jérôme B. Eur Phys J E 2003;12:383.
[49] Green PF, Ganesan V. Eur Phys J E 2003;12:449.
[50] Sferrazza M, Xiao C, Jones RAL. Phys Rev Lett 1997;78:3693.